

Effect of Allium Cepa on the Properties of Nickel Doped Zinc Oxide Nanopyramids

¹Ijeh R., *²Samson O. A., ²Ezema F. I., ³Asarhasa P.

¹Department of Physics, University of Delta, Agbor, Delta state, Nigeria

²Department of Physics and Astronomy, University of Nigeria Nsukka, Nigeria

³Department of Physics, Delta State College of Education, Warri, Delta state, Nigeria

*Corresponding author's email: samson.aisida@unn.edu.ng Phone: +2348063957679

ABSTRACT

The biosynthesis protocol of functional oxide like Zinc oxide nanoparticles has gained serious momentum in nanomedicine. Nickel doped Zinc oxide in the solution of allium cepa has been employed in this work. The AC serves as a potential reducing agent. The surface morphology of the formulated sample was obtained using scanning electron microscope (SEM) which revealed pronounced crystals of nanopyramid shape with increase in concentration of reducing agent, the X-ray diffraction (XRD) spectroscopy revealed a single phase characteristic of the sample and the Fourier transform infrared (FTIR) result revealed the presence of functional groups and chemical bonding which culminated into a shift from higher wave number to a lower wave number. The obtained properties of the formulated samples were influenced by the AC concentration. It is remarkable that the AC-NiZnONPs sample formulated is propitious for potential biomedical application..

Keywords:

Nanoparticles,
Zinc oxide,
Nanopyramids,
Allium cepa.

INTRODUCTION

Zinc Oxide (ZnO) is a promising metal oxide that exhibits structures such as hexagonal wurtzite, rock salt and zinc composite at room temperature (Ebrahimi *et al.*, 2012). ZnO is an n-type semiconductor that is odorless, non-toxic, chemically stable, environmentally friendly and soluble in acids and alkali. It is notable for good thermal conductivity, high electron mobility, good transparency with wide bandgap of 3.37 eV (Kalam *et al.*, 2022; Ali *et al.*, 2018). Zinc Oxide nanoparticle (ZnO-NP) is a very prominent inorganic semiconductor material that has been extensively investigated compared to other nanoparticles due to the facilitating physical and chemical properties (Mishra *et al.*, 2017). The high surface to volume ratio of ZnO-Np has contributed for easy disintegration for catalysts application (Deka *et al.*, 2022). It is evident that recently, interest of researchers is shifting from applications of nanoparticles in electronics towards nanomedicines. The therapeutic potency of doped ZnO-NPs is high as it properly modulates systemic circulation in patients thereby improving the quality of life by minimizing side effects. The doping of ZnO with Nickel has predominantly attracted attention due to improved properties of ZnO nanoparticles. In this work, we adopted green method for the deposition of ZnO-NPs which has been adjudged as convenient,

inexpensive, reliable and sustainable technique for the preparation of NPs and also environmentally friendly (Barzinjy, 2022). Doped ZnO-NPs has some feasible applications in biomedical research for the transportation of drugs to the active site of the target at a given rate and sustained for a stipulated time (Mohanraj and Chen, 2006). The process of delivery which is usually aimed at inhibiting growth of bacteria in patients, diabetes and for combating spread and subsistence of cancerous cells through nanotherapy without causing harm to the cells (Bloh *et al.*, 2021; Gowda *et al.*, 2013). Furthermore, Ni-ZnO-NP discharges zinc ions easily due to the sufficiency of –OH and contributes to the production of reactive oxygen species (ROS) that improve the level of antioxidant and energy needed to power the cells (Hu *et al.*, 2019; Choudhury *et al.*, 2017). It also stabilizes the free radicals capable of proteins and cells damages during metabolic process in the body.

Several methods that have been used for the synthesis of Ni-doped Zinc oxide include sol-gel (Kim *et al.*, 2008), spray pyrolysis (Bouaoud *et al.*, 2013), radio frequency ((Gholami *et al.*, 2020), metal organic chemical vapour (Gholami *et al.*, 2020), Furthermore, researchers like (Rana and Singh, 2016; Faye *et al.*, 2022) studied antibacterial activities of Ni doped Zinc oxide using extract of Euphorbia abyssinica. In this work we

decided to use *Allium cepa* as a potential reducing agent for the synthesis of ZnO-NPs.

Allium cepa also known as onion is an agricultural crop that belongs to the family of *Amaryllidaceae* used as flavor in meals. For some decades, *Allium cepa* has also been tremendously used as medicinal herbs for the treatment of diseases, healing wounds, and combating pneumonia, high blood pressure reduction and management of diabetes (Ahmed *et al.*, 2015; Galavi *et al.*, 2021). Pharmacologically, it has shown that stomach and intestinal disorders are relieved off and improves appetite when *Allium cepa* is consumed in moderate quantity (Kumar *et al.*, 2010). Agricultural produce such as plants are good candidates for the synthesis of nanoparticles by process of reduction. *Allium cepa* is a formidable plant with extracts used as reducing and coating agents for the reduction of ions in deposited samples. Furthermore, any method that uses extract of *Allium cepa* ensures reduction of environmental pollution problems.

This work involves biosynthesis protocol for the formulation of NiZnONPs using AC solution as a good reducing agent. The influence of *Allium cepa* (AC) will be observed on the properties of the formulated samples. The obtained sample will be useful for biomedical applications.

Materials and methods

Analytical grade of Zinc nitrate hexahydrate (98%) and Nickel nitrate hexahydrate (99%) were purchased commercially (Sigma-Aldrich products). *Allium cepa* (AC) was obtained from a local market and used as a potential reducing and stabilizing agent. All the chemicals were used without further purification and distilled water was used for all the synthesis procedures.

Preparation of AC-Ni-ZnO nanocomposite

Zinc nitrate (0.10 M) and Nickel nitrate (0.010 M) were homogenized in 100 mL DW under continuous stirring at 600 rpm for 1h. These procedures were reported four times, to the second, third and fourth solutions, 30, 50 and 80 mL aqueous extract of AC were added drop wise and a colour change was observed under continuous stirring for another 1 h respectively. The formed precipitate was then heated at 60 °C under stirring at 600 rpm for another 4 h to form gel. The formed gel was dried at 100 °C for 4 h in a muffle oven followed by sintering at 300, 500 and 700 °C for 3 h in a hot air vacuum tube furnace. The as-prepared sample and the

samples with 30, 50 and 80 mL aqueous extract of AC were labelled as B₁, B₂, B₃ and B₄ respectively for the various characterizations and applications.

Characterizations

An X-ray diffractometer (XRD) model PW 3710/PW1710 from PHILIPS was used to determine the structural analysis of the samples in the 10° to 100° range at room temperature. Fourier transform infrared spectroscope (FTIR) model PERKIN ELMER SPECTRUM 100 in the range of 400 – 4000 cm⁻¹ to identify the chemical bonds in the molecules of the samples.

A Scanning electron microscope (SEM), Nova Nano SEM 450 (FEI Company) was used to determine the surface morphology. Energy dispersive spectroscopy (EDS) coupled to the SEM machine was used to determine the elemental compositions of the samples.

RESULTS AND DISCUSSION

SEM and EDX analysis

Figure 1 shows the SEM micrographs of the samples. The as-prepared sample shows a shape that is not fully spherical in shape. The pyramidal shape of the sample was submerged by the spherical shape as seen in Fig. 1(a). The pyramidal shape became more obvious with the addition of 20% per volume of the reducing agent as seen in Fig. 1(b). As the concentration of the reducing agent increases to 50%, the observed shape was seen in a better shape as seen in Fig. 1(c). As soon as the concentration of the reducing agent increased to 80%, the pyramid shape was seen clearly as seen in Fig. 1(d). This shows that the reducing agent played a vital role in the formation of the nanopyramid. Similar result was observed by (Aisida, et al., 2021) with zinc ferrite. The elemental compositions of the samples determined by EDS is presented in figure 2. Strong absorption peaks at ≈ 1.2 keV and 2.6 keV was observed for Zn and Ni respectively. Other obvious peak is O. The observed C we adduced to the reducing agent in the sample. The elemental compositions of the samples were detected by Electron Diffraction X-ray (EDX) as shown in Fig.3. It was observed that Zn showed stronger absorption peaks at 1.2 keV as the reducing concentration increases for both the undoped and doped samples compared to Nickel at 2.6 keV. The observed C we adduced to the reducing agent in the sample.

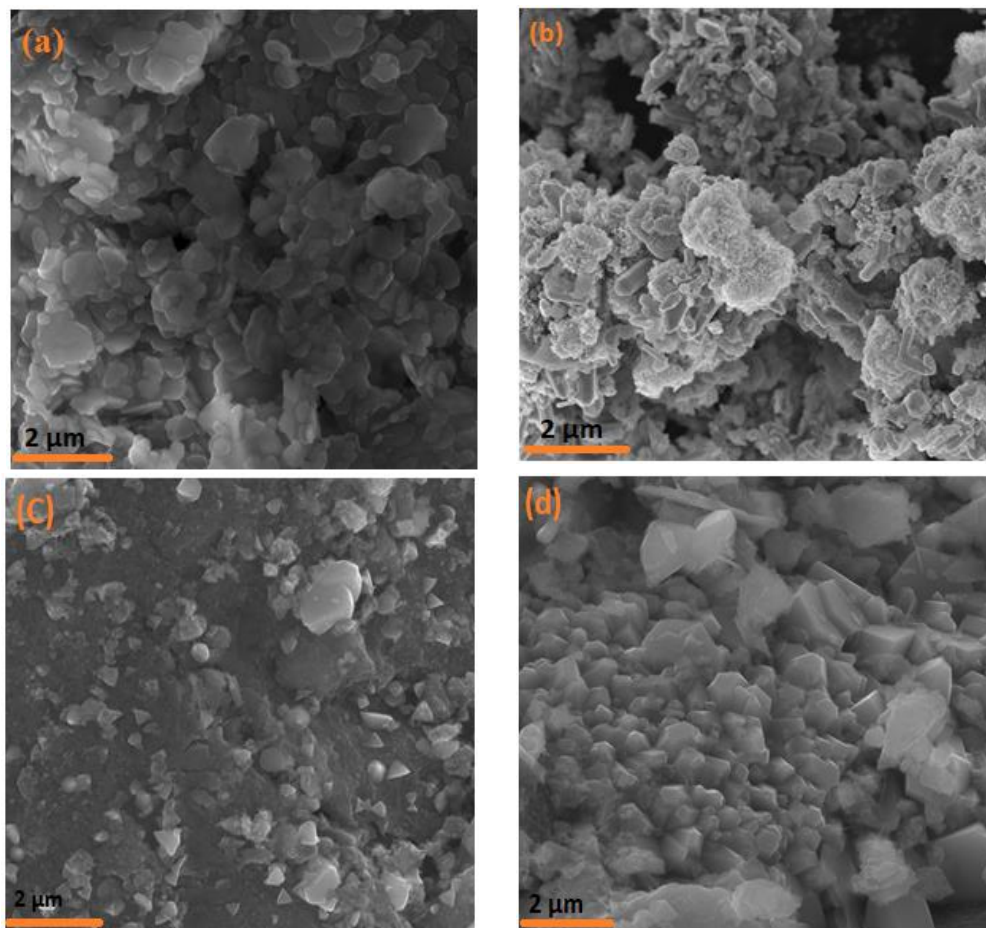


Figure 1: SEM result of Ni-ZnO:AC (a) 80:0 (b) 80:20 (c) 80:50 (d) 80:80

XRD analysis

The XRD analysis of the samples as shown in figure 3 gives a crystalline structure of the samples with the highest peak observed at (311) plane. The diffraction peaks with their crystallographic planes observed at 2θ value for all the samples are 30.2° (220), 35.5° (311), 43.4° (400), 53.5° (422), 57.2° (511) and 62.8° (340) showing the single phase characteristic of the sample in their inverse spinel lattice structure. The crystallite size

of the sample was analyzed using the Debye–Scherer's formula Eq. (1). The results are presented in table 1. Similar result was observed by (Aisida, et al., 2021) with zinc ferrite.

$$\Phi_{(XRD)} = \frac{0.9\lambda}{\beta \cos\theta} \quad (1)$$

where $\Phi_{(XRD)}$ is the crystallite size (nm), λ is the X-ray wavelength ($\lambda = 1.5406 \text{ \AA}$), β is the full width at half maximum (FWHM) intensity measured in radians.

Table 1: Showing the evaluation of the crystallite size of Ni-ZnO:AC

Samples	2 theta	FWHM	$\Phi_{(XRD)}$
a	35.54913	0.41703	20.8
b	35.52313	0.46031	18.9
c	35.54913	0.46558	18.7
d	35.52313	0.39452	20.0

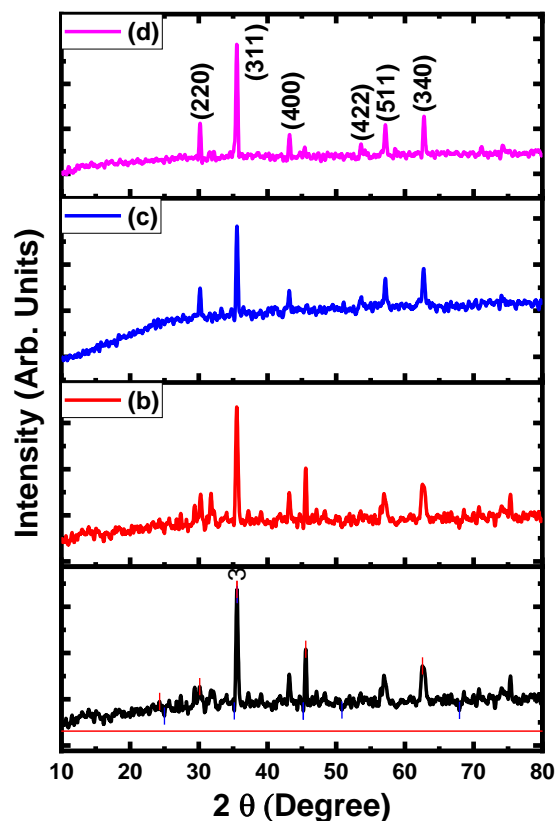


Figure 2: XRD result of Ni-ZnO:AC (a) 80:0 (b) 80:20 (c) 80:50 (d) 80:80

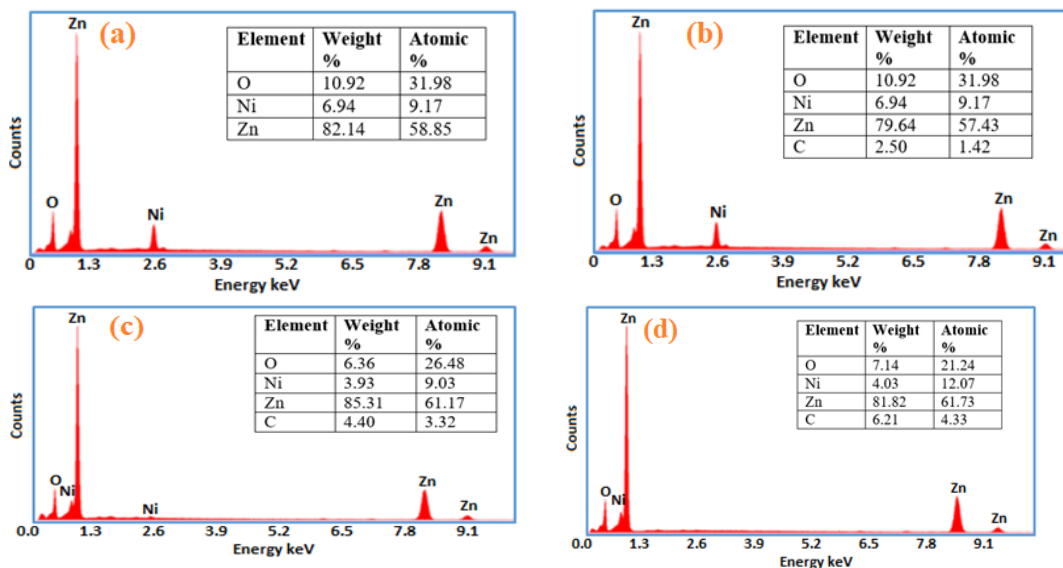


Figure 3: EDX analysis of Ni-ZnO:AC (a) 80:0 (b) 80:20 (c) 80:50 (d) 80:80

FTIR analysis

The Fourier transform infrared spectroscopy was used to analyze the functional properties of the samples as shown in Fig. 4. The various vibrations (i.e. stretching and bending) were revealed in the wavelength range of 3500 – 400 cm⁻¹ (Aisida *et al.*, 2022). The stretching

vibration associated with O-H group ranges from 3325 to 3390 cm⁻¹. We observed a shift from higher wave number to a lower wave number from sample “a” to “d”. This stretching which result to the decrease in wave number could be due to effect of absorbance in the extract as a result of the Proteins group. The stretching

band that ranges between 1574 to 1583 cm^{-1} is linked to C = O functional group. A shift from higher wave number to a lower wave number from sample "a" to "d" was also observed. C-N stretching functional group was observed to vary from 1502 to 1504 cm^{-1} . The observed shift in this group was mild and this might be as a result of the aromatic amines organic molecules in the extract.

The band observed at 830 cm^{-1} for all the samples is associated with C-O-C stretching vibration functional group. There was no observable shift in this group for all the samples. The observed band is owing to the ethers organic molecules in the samples. The observed band at 537 cm^{-1} is linked to ZnO surfaces (Aisida *et al.*, 2019).

Table 2: The functional group of Ni-ZnO:AC

Functional group	Wavelength (cm^{-1})				Organic molecules
	(a)	(b)	(c)	(d)	
OH (symmetric stretching)	3390	3360	3349	3325	Phenol/ aromatic
C=O (Asymmetric stretching)	1583	1574	1574	1574	Proteins
C-N stretching	1502	1504	1504	1504	aromatic amines
C-O-C bending	830	830	830	830	Ethers
Zn-O stretching	537	537	537	537	metal oxide

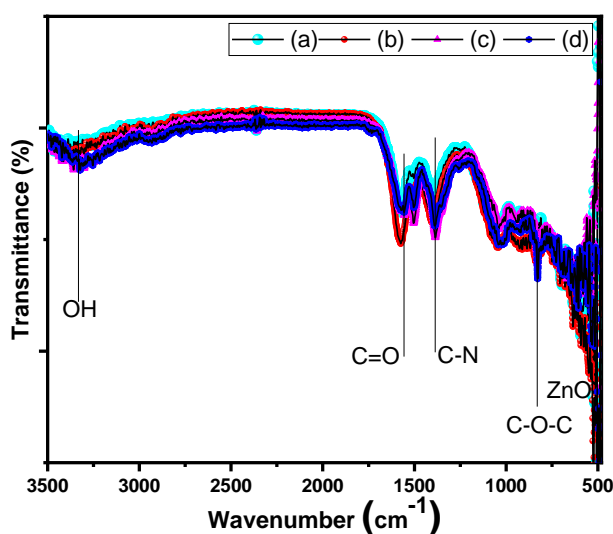


Figure 4: FTIR result of Ni-ZnO:AC (a) 80:0 (b) 80:20 (c) 80:50 (d) 80:80

CONCLUSION

The AC serves as a potential reducing agent. The SEM results shows pronounced crystals of nanopyramid shape with increase in concentration of reducing agent, the XRD revealed a single phase characteristic of the sample and the FTIR result revealed the presence of functional groups and chemical bonding which culminated into a shift from higher wave number to a lower wave number. The obtained properties of the formulated samples were influenced by the AC concentration. It is remarkable that the AC-NiZnONPs formulated is propitious for potential biomedical application.

REFERENCES

Ahmed, N., Mahmood, A., Ashraf, A., Bano, A., Tahir, S. S., and Mahmood, A. (2015) "Ethnopharmacological relevance of indigenous medicinal plants from district Bahawalnagar, Pakistan,," *Journal of Ethnopharmacology*

Aisida, S. O., Madubuonu, N., Alnasir, M. H., Ahmad, I., Botha, S., Maaza, M., and Ezema, F. I. (2019) "Biogenic synthesis of iron oxide nanorods using Moringa oleifera leaf extract for antibacterial applications," *Applied Nanoscience*. <https://doi.org/10.1007/s13204-019-01099-x>.

Aisida, S. O., Onwujiobi, C., Ahmad, I., Zhao, T.k., Maaza, M., and Ezema, F. I. (2022) "Biogenic synthesis of zinc oxide nanorods for biomedical applications and photodegradation of Rhodamine B," *Materials Today Communications*, 33, 104660.

Aisida, S.O, Ali, A., Ahmad, I., Ul-Hamid, A., Zhao, T., Maaza, M., Ezema, F.I. (2021) "Biogenic synthesis of Allium cepa induced structural, morphological, magnetic, optical and thermoablation properties of zinc ferrite nanoparticles" *Journal of nanoparticle research*, 23, 47

- Ali, R. N., Naz, H., Li, J., Zhu, X., Liu., P. and Xiang, B. (2018) "Band gap engineering of transition metal (Ni/Co) codoped in zinc oxide (ZnO) nanoparticles," *Journal of Alloys and Compounds*, 744, 90-95.
- Barzinjy, A. A., Mustafa, S., Hamad, S., and Hamad, A. H. (2022) "Green synthesis of Ni doped ZnO nanoparticles using dandelion leaf extract and its solar cell applications," *Ceramics International*, 48, (19), 29257-29266
- Bloh, A., Naji, H. K., and Obead, A. R. (2021) "Novelty Predictor ZnO Nano practical for Cancer Treatment," *Indian Journal of Forensic Medicine & Toxicology*, 15 (4), 686-690.
- Bouaoud, A., Rmili, A., Ouachtari, F., Louardi, V., Chtouki, T., Elidrissi, B., and Erguig, H. (2013) "Transparent conducting properties of Ni doped zinc oxide thin films prepared by a facile spray pyrolysis technique using perfume atomizer," *Materials Chemistry and Physics*, 137(3), 843-847
- Choudhury, S., Ordaz, J., Lo, C.L., Damayanti, N. P., Zhou, F., and Irudayaraj, J. (2017) "Zinc oxide Nanoparticles-Induced Reactive Oxygen Species Promotes Multimodal Cyto-and Epigenetic," *Toxicity Toxicological sciences*, 156, 261-274
- Deka, B., Baruah, C., Babu, A., and Kalita, P. (2022) "Biological and Non-Conventional Synthesis of Zinc Oxide Nanoparticles (ZnO-NPs): Their Potential Applications," *Journal of Nanotechnology Nanomaterials*, 3, 79-89.
- Ebrahimi, H., Modrek, M., and Mozaffari, M. (2012) "Photo Degradation of Direct Red 81 (5-Solamine) by using zinc oxide nanoparticles on glass granule substrate in acidic pH and various atmospheres.," *World Applied Sciences Journal*, 19, 352–354.
- Faye, G., Jebessa, T., and Wubalem, T. (2022) "Biosynthesis, characterisation and antimicrobial activity of zinc oxide and nickel doped zinc oxide nanoparticles using *Euphorbia abyssinica* bark extract," *IET Nanobiotechnology*, 16, 25-32.
- Galavi, A., Hosseinzadeh, H., and Razavi, B. M. (2021) "The effects of *Allium cepa* L. (onion) and its active constituents on metabolic syndrome: A review," *Iran Journal of Basic Medical Sciences*, 24, 3-16.
- Gholami, M., Rasoulzadeh, H., Ahmadi, T., and Hosseini, M. (2020) "A Synthesis, characterization of Nickel doped Zinc oxide by radio-frequency sputtering and application in photo-electrocatalysis degradation of Norfloxacin," *Materials Letters*, 269, 127647.
- Gowda, R., Jones, N., Banerjee, S., and Robertson, G. (2013) "Use Of Nanotechnology to Develop Multi-Drug Inhibitors for Cancer Therapy.," *Journal of Nanomedicine & Nanotechnology*, 1(4), 61000184
- Hu, Y., Zhang, H. R., Dong, L., Xu, M. R., Zhang, L., Ding, W. P., Zhang, J. Q., Lin, J., Zhang, Y. J., and Qiu, B. S. (2019) "Enhancing tumor chemotherapy and overcoming drug resistance through autophagy-mediated intracellular dissolution of zinc oxide nanop," *Nanoscale*, 11, 11789-11807.
- Kalam, A., Allami, S., Al-Sehemi, A., Assiri, M., and Yadav, P. (2022) "Effect of Stabilizer on Optical band gap of ZnO and their performance in Dye-sensitized Solar cells," *Journal/Bulletin of the Chemical Society of Ethiopia*, 36, 209-222.
- Kim, K.T., Kim, G.H., Woo, J.C., and Kim, C.I. (2008) "Characteristics of Nickel-doped Zinc Oxide thin films prepared by sol-gel method," *Surface & Coatings Technology*, 202, 5650-5653
- Kumar, K. P. S., Bhowmik, D., Biswajit, C., and Tiwari, P. (2010) "*Allium cepa*: A traditional medicinal herb and its health benefits," *Journal of Chemical and Pharmaceutical Research*, 2, 283-291.
- Manzoor, Z., Saravade, V., Corda, A. M., Ferguson, I., and Lu, N. (2020) "Optical and Structural Properties of Nickel Doped Zinc Oxide Grown by Metal Organic Chemical Vapor Deposition (MOCVD) at Different Reaction Chamber Conditions ES," *Materials & Manufacturing*, 8, 31-35.
- Mishra, P. K., Mishra, H., Ekielski, A., Talegaonkar, S., and Vaidya, B. (2017) "Zinc oxide nanoparticles: a promising nanomaterial for biomedical applications," *Drug Discovery Today*, 22, 1825-1834.
- Mohanraj, V., and Chen, Y. (2006) "Nanoparticles – A review.," *Tropical Journal of Pharmaceutical Research*, 5, 561-573.
- Rana, S. and Singh, R. (2016) "Investigation of structural, optical, magnetic properties and antibacterial activity of Ni-doped zinc oxide nanoparticles.," *Journal of Materials Science: Materials in Electronics*, 27, 9346–9355